



# City Research Online

## City, University of London Institutional Repository

---

**Citation:** Sedhain, S. & Giaralis, A. (2019). Enhanced optimal tuned mass-damper-inerter performance for seismic protection of multi-storey buildings via top-storey softening. Paper presented at the SECED 2019 Conference, 9-10 September 2019, Greenwich, London.

This is the accepted version of the paper.

This version of the publication may differ from the final published version.

---

**Permanent repository link:** <https://openaccess.city.ac.uk/id/eprint/24469/>

**Link to published version:**

**Copyright:** City Research Online aims to make research outputs of City, University of London available to a wider audience. Copyright and Moral Rights remain with the author(s) and/or copyright holders. URLs from City Research Online may be freely distributed and linked to.

**Reuse:** Copies of full items can be used for personal research or study, educational, or not-for-profit purposes without prior permission or charge. Provided that the authors, title and full bibliographic details are credited, a hyperlink and/or URL is given for the original metadata page and the content is not changed in any way.

---

---



## ENHANCED OPTIMAL TUNED MASS-DAMPER-INERTER PERFORMANCE FOR SEISMIC PROTECTION OF MULTI-STORY BUILDINGS VIA TOP-STORY SOFTENING

Sailesh SEDHAIN<sup>1</sup> and Agathoklis GIARALIS<sup>2</sup>

**Abstract:** The tuned-mass-damper-inerter (TMDI) is a linear passive dynamic vibration absorber for the seismic protection of buildings. It couples the tuned-mass-damper (TMD), comprising an oscillatory secondary mass installed at top building floor via a spring and a damper, with an inerter device developing acceleration-dependent resisting force. In the TMDI configuration, the inerter connects the secondary mass to a lower than the top floor and recent work established that the more floors the inerter spans the more effective the TMDI becomes over the TMD. Recognizing that spanning more than one floors may not be practically appealing in low-to-midrise buildings due to increased space utilization requirements, this paper examines the seismic performance of TMDI-equipped buildings with inerter spanning only one (the top) floor upon softening the top floor. Numerical results pertaining to a linear 10-storey shear frame structure demonstrate that TMDIs spanning one floor ("1" TMDI) are more effective than TMDIs spanning two floors ("2" TMDI) upon top-floor softening by 80%. This is shown by considering "-1" and "-2" TMDIs with wide range of inertial properties optimally tuned to minimize penultimate floor deflection variance for coloured stationary excitation compatible with the Eurocode 8 response spectrum. Moreover, improved performance of "-1" TMDI with top floor softening compared to "-2" TMDI by 85% or more is found in terms of root-mean-square and peak values for penultimate floor deflection, storey drift, and acceleration by considering response history analyses to optimal TMDI-equipped structures for a suite of 7 ground motions spectrally matched to Eurocode 8 response spectrum. It is concluded that the herein proposed structural modification (top-floor softening) may improve significantly the seismic performance of TMDI-equipped building structures.

**Keywords:** tuned mass-damper-inerter; response spectrum compatible stochastic excitation; passive seismic vibration control

### Introduction

The use of passive linear tuned mass-damper (TMD) has been considered as a viable solution for the protection of building structures exposed to earthquakes for quite some time (e.g., Villaverde and Koyama 1993, Sadek et al. 1997, Pinkaew et al. 2003). In its simplest form, the TMD comprises an oscillating mass attached to the top floor of the building whose vibration motion is to be controlled (primary structure) via optimally designed/"tuned" linear spring and damper elements. The functionality of the TMD relies on "tuning" its stiffness and damping properties for a given primary structure and attached mass, such that significant kinetic energy is transferred from the primary structure to the TMD mass and dissipated through the viscous damper. No matter the performance criterion adopted in this design, it is widely recognized that the TMD effectiveness for seismic hazard mitigation of structures depends heavily on its inertia properties: the larger the attached TMD mass, the more effective the TMD is in mitigating seismically induced oscillations (e.g., Hoang et al. 2008, De Angelis et al. 2012, Moutinho 2012).

In this regard, the tuned mass-damper-inerter (TMDI) configuration, first introduced by Marian and Giaralis (2013, 2014), has been shown to be quite advantageous over the TMD in controlling earthquake induced vibrations in multi-storey buildings in a number of recent studies (Giaralis and Taflanidis 2015 and 2018, Ruiz et al. 2018, Taflanidis et al. 2019) by relying on the mass amplification effect of the inerter. The latter is a two-terminal device developing a resisting force

<sup>1</sup> PhD Candidate, City University London, London, United Kingdom

<sup>2</sup> Senior Lecturer in Structural Engineering, City University of London, London, United Kingdom, [agathoklis@city.ac.uk](mailto:agathoklis@city.ac.uk)

proportional to the relative acceleration of its terminals by a constant of proportionality termed inertance and measured in mass units (Smith 2002). In the TMDI configuration, the inerter is utilized to connect the top-floor attached mass to a different (lower) floor. This consideration endows additional inertia property to the attached mass through the inertance without increasing the overall attached weight as the inertance can be several orders of magnitude larger than the physical mass of the inerter device (e.g., Papageorgiou et al 2008, Nakaminami et al 2016). In this context, it was shown numerically by Giaralis and Taflanidis (2015, 2018) that optimally designed TMDIs are considerably more efficient in reducing seismic structural demand than TMDs when the inerter spans more than one floors (see also Giaralis and Petrini 2017). However, such TMDI configurations may not be practically appealing in low-to-mid-rise buildings as they use space within the structure in more than one (the top) floor. To this end, herein, a novel approach is proposed and numerically exemplified for the seismic protection of TMDI-equipped multi-storey building structures in which the top floor is purposely designed to be significantly softer from the rest of the building floors. This modification of the primary structure aims to bring about enhanced mass amplification inerter effect in TMDIs where the inerter spans only one floor (i.e., taking space only from the top floor).

The remainder of the paper is organized as follows. First, the proposed TMDI configuration with top-floor softening is introduced and discussed vis-à-vis previously explored TMDI configurations. Next, mathematical details of a standard optimal TMDI design approach are reviewed aiming to minimize peak displacement of the penultimate (unsoftened) floor. This consideration ensures that performance enhancement is fairly evaluated with regards to a regular in elevation structure. Then, optimal TMDI designs with unsoftened top floor and inerter spanning one and two floors as well as with softened top floor and inerter spanning only one floor are obtained in a benchmark 10-storey shear frame building structure subject to Eurocode 8 compatible stationary ground excitation. Lastly, additional data from response history analyses for a suite of Eurocode 8 spectrum compatible accelerograms are reported gauging the effectiveness of top-floor softening in TMDI-equipped structures to reduce penultimate floor displacement, acceleration as well as inter-story drift and pertinent conclusions are summarized.

## Modelling of TMDI-equipped multi-storey buildings

Consider a  $n$ -storey building whose lateral response to horizontal ground acceleration excitation,  $a_g$ , can be faithfully modelled through a linear damped  $n$  degree-of-freedom (nDOF) frame-like structure with lumped floor masses  $m_k$ ;  $k=1,2,\dots,n$  as shown in Figure 1(a). A TMDI located at the top floor of the building is herein used to suppress lateral floor deflections,  $x_k$ . It consists of a conventional TMD comprising a secondary  $M_{TMDI}$  mass attached to the top floor via a stiffener, modelled as a linear spring with  $K_{TMDI}$  stiffness, in parallel with a linear viscous damper, modelled as a dashpot with damping coefficient  $C_{TMDI}$ , and an inerter device, highlighted in red in Figure 1, connecting the secondary mass to  $p$  floors below the top floor (" $-p$ " TMDI connectivity).

In this work, the inerter device is modelled through an ideal massless mechanical element resisting the relative acceleration developing at its two ends/terminals through the inertance coefficient  $b$  (Smith 2002). In this regard, the inerter element force reads as

$$F = b(\ddot{x}_{TMDI} - \ddot{x}_{n-p}), \quad (1)$$

where  $x_{TMDI}$  is the lateral deflection of the TMDI mass and a dot over a symbol denotes differentiation with respect to time  $t$ . For illustration, the inset of Figure 1(b) isolates the inerter element for the special case of " $-1$ " TMDI connectivity originally treated by Marian and Giaralis (2013, 2014). Therefore, in the TMDI configuration the inerter exerts an additional, compared to the conventional TMD, control force,  $F$ , to the host structure whose amplitude depends on the relative acceleration of the inerter terminals and on the inertance  $b$ . In this regard, Marian and Giaralis (2013, 2014) showed that TMDI achieves improved vibration suppression capability in seismically excited multi-storey structures through increasing inertance  $b$ . More recently, Giaralis and Taflanidis (2015, 2018) demonstrated numerically that improved earthquake-induced vibration suppression is also achieved by TMDI configurations in which the inerter spans more than one floors (i.e.,  $p>1$ ). For example, Figure 1(c) shows the case of  $p=2$  (i.e., " $-2$ " TMDI connectivity). Nevertheless, as discussed in the introduction, TMDI configurations for  $p>1$  may not be practically appealing as they involve increased inerter installation costs as well as giving up valuable space in more than the top building floor. To this end, it is herein proposed to increase the relative acceleration at the ends of the inerter, and therefore TMDI vibration suppression

effectiveness, not by spanning more floors but by softening the top floor of the host structure. The latter can be practically achieved by reducing the dimensions of the top storey columns (as graphically shown in Figure 1(d)) and/or by increasing the top storey height. In the numerical part of this paper, the latter setting (i.e., TMDI “-1” with top floor softening) is compared with TMDI “-1” and “-2” without top floor softening. Importantly, the basis of comparison is to examine seismic demands of the penultimate storey of the TMDI-equipped structure vis-à-vis the uncontrolled structure with no top-floor softening. This provision ensures that top-floor softening is not seen as an artificial weakening of the primary/host structure which the TMDI retrofits but, rather, as a purpose-made modification to the host structure to achieve an overall better seismic performance of the TMDI-equipped building.

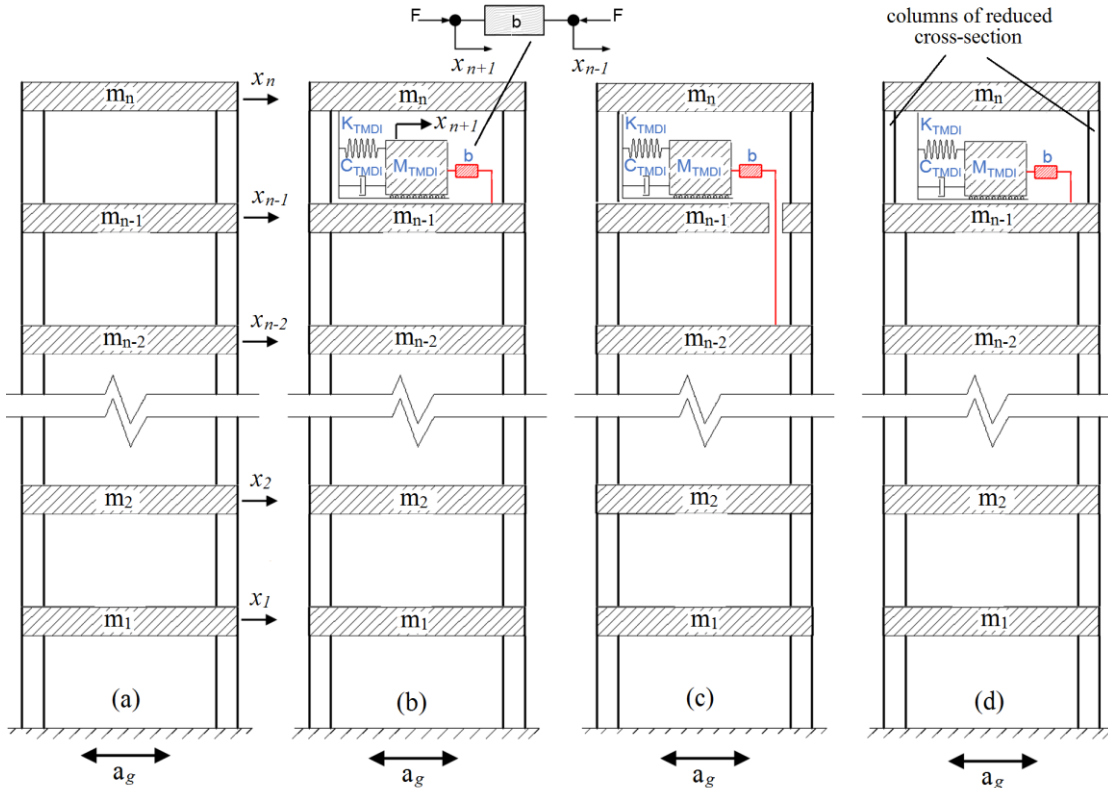


Figure 1 Considered TMDI configurations: (a) uncontrolled structure; (b) TMDI “-1” connectivity; (c) TMDI “-2” connectivity; (d) TMDI “-1” connectivity with top floor softening (proposed configuration)

Mathematically, the  $n+1$  equations of motion of a top-floor TMDI-equipped nDOF frame-like dynamical system subject to ground acceleration,  $a_g(t)$ , can be written in matrix form as

$$\mathbf{M}\ddot{\mathbf{x}}(t) + \mathbf{C}\dot{\mathbf{x}}(t) + \mathbf{K}\mathbf{x}(t) = -\mathbf{M}_o\boldsymbol{\delta}a_g(t). \quad (2)$$

In the last expression,  $\mathbf{x}(t) \in \mathbb{R}^{(n+1)\times 1}$  is a vector collecting all  $x_k$  floor deflections as well as the TMDI deflection  $x_{TMDI}$ , while  $\boldsymbol{\delta} \in \mathbb{R}^{(n+1)\times 1}$  is the unit vector. Further,  $\mathbf{M}$ ,  $\mathbf{C}$ , and  $\mathbf{K}$  are the mass, damping and stiffness matrix, respectively, of the TMDI-equipped nDOF system given as

$$\begin{aligned} \mathbf{M} &= \mathbf{M}_s^{n+1} + (m_{TMDI} + b)\mathbf{1}_{n+1}\mathbf{1}_{n+1}^T + b\mathbf{1}_{n-p}\mathbf{1}_{n-p}^T - b(\mathbf{1}_{n+1}\mathbf{1}_{n-p}^T + \mathbf{1}_{n-p}\mathbf{1}_{n+1}^T) \\ \mathbf{C} &= \mathbf{C}_s^{n+1} + C_{TMDI}(\mathbf{1}_{n+1}\mathbf{1}_{n+1}^T + \mathbf{1}_n\mathbf{1}_n^T - \mathbf{1}_{n+1}\mathbf{1}_n^T + \mathbf{1}_n\mathbf{1}_{n+1}^T) \\ \mathbf{K} &= \mathbf{K}_s^{n+1} + K_{TMDI}(\mathbf{1}_{n+1}\mathbf{1}_{n+1}^T + \mathbf{1}_n\mathbf{1}_n^T - \mathbf{1}_{n+1}\mathbf{1}_n^T + \mathbf{1}_n\mathbf{1}_{n+1}^T) \end{aligned} \quad (3)$$

while  $\mathbf{M}_o$  is equal to  $\mathbf{M}$  for  $b=0$ . In Eq.(3),  $\mathbf{M}_s^{n+1} \in \mathbb{R}^{(n+1)\times(n+1)}$ ,  $\mathbf{C}_s^{n+1} \in \mathbb{R}^{(n+1)\times(n+1)}$ , and  $\mathbf{K}_s^{n+1} \in \mathbb{R}^{(n+1)\times(n+1)}$  are the mass,  $\mathbf{M}_s \in \mathbb{R}^{n\times n}$ , the damping,  $\mathbf{C}_s \in \mathbb{R}^{n\times n}$ , and the stiffness,  $\mathbf{K}_s \in \mathbb{R}^{n\times n}$ , matrices of the uncontrolled structure in Figure 1(a), respectively, augmented by one last (bottom) row with zero entries and by one last (rightmost) column with zero entries. Further, the vector

$\mathbf{1}_p \in \mathbb{R}^{(n+1) \times 1}$  has zero element except from the p-th entry which is equal to one, and the superscript “T” denotes matrix transposition. Note that for  $b=0$  (no inerter), Eqs. (2) and (3) represent the host building model with a conventional top-floor TMD widely considered for seismic protection of building structures (e.g., De Angelis et al. 2012). Further, for  $M_{TMDI}=0$  (no secondary mass), Eqs. (2) and (3) represent the host building model with a top-floor tuned inerter damper (TID), proposed by Lazar et al. (2014) for earthquake-induced vibrations suppression. Therefore, in the ensuing numerical work, top floor TMD and TID are treated as special cases of the TMDI by setting  $b=0$  and  $M_{TMDI}=0$ , respectively.

### Optimal TMDI design: problem formulation

Let the ground acceleration excitation  $a_g$  in Eq. (2) be modelled as stationary stochastic process. Following the work of Marian and Giaralis (2013, 2014), TMDI is herein designed for fixed host structure (with or without top floor softening) such that the response variance of the penultimate floor,  $n-1$ , is minimized for reasons discussed in the previous section. The TMDI design is cast as an optimization problem involving four dimensionless design parameters, namely the TMDI frequency and damping ratios defined as

$$\nu_{TMDI} = \frac{\sqrt{K_{TMDI}}}{\omega_1} \quad \text{and} \quad \zeta_{TMDI} = \frac{C_{TMDI}}{2\sqrt{(M_{TMDI} + b)K_{TMDI}}}, \quad (4)$$

respectively, where  $\omega_1$  is the first natural frequency of the uncontrolled structure, and grouped in the vector  $\mathbf{u}_1 = [\nu_{TMDI} \quad \zeta_{TMDI}]^T$ , as well as the mass and inertance ratios defined as

$$\mu = \frac{M_{TMDI}}{M_{tot}} \quad \text{and} \quad \beta = \frac{b}{M_{tot}}, \quad (5)$$

respectively, where  $M_{tot}$  is the total mass of the uncontrolled structure, grouped in the vector  $\mathbf{u}_2 = [\mu \quad \beta]^T$ . The objective function (OF) to be minimized is defined as

$$\sigma^2 = \int_0^\infty |H_{n-1}(\omega)|^2 G(\omega) d\omega, \quad (6)$$

where  $G(\omega)$  is the one-sided power spectral density function (PSD) representing the  $a_g$  process in the frequency domain and  $H_{n-1}$  is the transfer function relating the (input) support excitation in terms of acceleration to the (output) relative displacement of the penultimate floor mass of the host building structure. This transfer function is given as

$$H_{n-1}(\omega) = \mathbf{C}_o (i\omega \mathbf{I}_{2n+2} - \mathbf{A})^{-1} \mathbf{B}, \quad (7)$$

where  $i=(-1)^{1/2}$ ,  $\mathbf{C}_o \in \mathbb{R}^{1 \times (2n+2)}$  is a row vector of zero elements except for the third element which is equal to 1,  $\mathbf{I}_{(q)}$  is the  $q$ -by- $q$  identity matrix, the superscript (-1) denotes matrix inversion, and matrices  $\mathbf{A} \in \mathbb{R}^{(2n+2) \times (2n+2)}$  and  $\mathbf{B} \in \mathbb{R}^{(2n+2) \times (2n+2)}$  are given as

$$\mathbf{A} = \begin{bmatrix} \mathbf{0}_{(n+1)} & \mathbf{I}_{(n+1)} \\ -\mathbf{M}^{-1}\mathbf{K} & -\mathbf{M}^{-1}\mathbf{C} \end{bmatrix} \quad \text{and} \quad \mathbf{B} = \begin{bmatrix} \mathbf{0}_{(n+1)} \\ \mathbf{I}_{(n+1)} \end{bmatrix} \quad (8)$$

respectively, where  $\mathbf{0}_{(q)}$  is the  $q$ -by- $q$  zero matrix. The optimization problem is solved numerically using a standard pattern search algorithm implemented in MATLAB® to determine design parameters in  $\mathbf{u}_1$  (primary design parameters) that minimize the adopted OF,  $\sigma$ , given values of the parameters in  $\mathbf{u}_2$  (secondary design parameters). The problem can be mathematically expressed as

$$\min_{\mathbf{u}_1} \left[ \sigma(\mathbf{u}_1 | \mathbf{u}_2) \right]. \quad (9)$$

Purposely, the above optimal design formulation allows for considering explicitly any desired combination of TMDI inertial properties, that is, attached mass and inertance, through the secondary design parameters  $\mu$  and  $\beta$ , respectively. In this manner, the special cases of the TMD ( $\beta=0$ ) and TID ( $\mu=0$ ) can be explicitly examined.

### Optimal TMDI design: numerical application for Eurocode 8 excitation

This section presents pertinent numerical results to probe into TMDI vibration suppression efficiency via top-floor softening of the host structure vis-à-vis TMDI configurations spanning more than one floor with no top floor softening. To this aim, the same host structure considered by Giaralis and Taflanidis (2015, 2018) is adopted as a case-study. The structure is a 10-storey linear classically damped planar shear frame. The lumped mass per story is 900ton whereas the inter-story stiffness decreases gradually along the frame height; it is 782.22MN/m for the bottom four stories, 626.10MN/m for the three intermediate ones and 469.57MN/m for the top three stories. The natural periods of the considered structure along with the participation factors in parenthesis are 1.5s (81.7%), 0.55s (11.8%), 0.33s (3.7%). Critical modal damping ratio of 5% is taken for all modes of vibration.

For TMDI optimal design, the PSD function,  $G(\omega)$ , plotted in Figure 2(a) is assumed to represent the seismic action. This PSD represents in the frequency domain a 20s-long stationary stochastic acceleration process which is compatible in the mean sense with the Eurocode 8 pseudo-acceleration response spectrum for peak ground acceleration (PGA) 0.36g ( $g=981\text{cm/s}^2$ ), ground type "B", and damping ratio 5% plotted in Figure 2(b) by thick gray line (BS EN 1998-1). The PSD is derived following the approach discussed in Giaralis and Spanos (2010a) and the achieved excellent level of compatibility with the target response spectrum is numerically verified in Figure 2(b) which superposes median spectral ordinates of an ensemble of 1000 20s-long stationary signals compatible with the PSD of Figure 2(a). These signals have been generated using a random field simulation technique based on an auto-regressive-moving-average filter (see e.g. Giaralis and Spanos 2009).

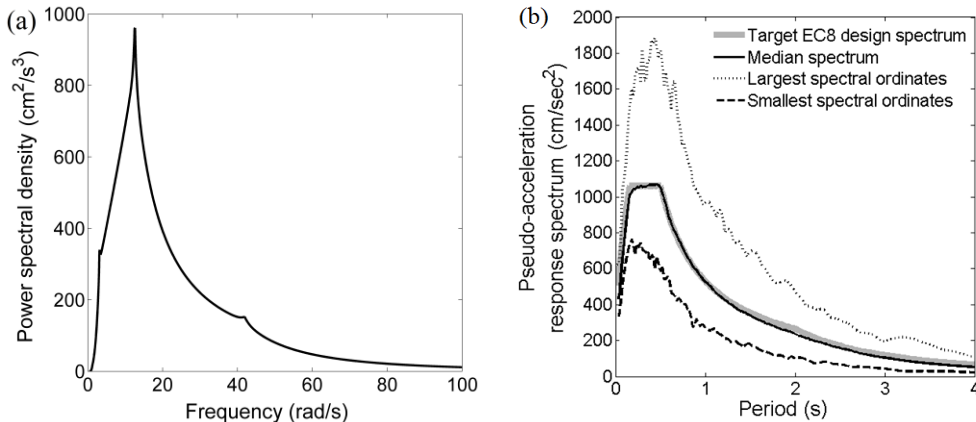


Figure 2 (a) Eurocode 8 compatible power spectral density (PSD) function for TMDI design (b) Numerical illustration of PSD compatibility to Eurocode 8 (target) response spectrum

The optimization problem of Eq. (9) is solved to derive optimum TMDI frequency and damping ratio parameters for the seismic PSD of Figure 2(a), for mass ratio  $\mu$  ranging within [0 5%] interval and for inertance ratio  $\beta$  ranging within [0 100%], and for the 3 different TMDI configurations shown in Figure 1(b-d). These are, “-1” and “-2” TMDIs with no top floor softening and a “-1” TMDI with 80% top storey stiffness reduction compared to the original 10-storey case-study structure. Note that the range of TMDI inertial properties examined are judiciously chosen to support a practically meaningful comparison of the three TMDI configurations.

Numerical results from optimal design of all three different TMDI configurations are reported in Figures 3 and 4 in the form of families of iso-value curves (one family for each configuration) plotted on the TMDI inertial design plane  $\mu\text{-}\beta$  of the secondary design parameters in  $\mathbf{u}_2$ . In these graphs, the y-axis corresponds to TMD optimal designs ( $\beta=0$ ), the x-axis corresponds to TID

optimal designs ( $M_{TMDI}=0$ ), and the origin corresponds to the uncontrolled structure. Figure 3 plots the optimal TMDI damping ratio,  $\zeta_{TMDI}$ , while Figure 4 plots the OF of the optimization problem, displacement variance  $\sigma^2$  of the penultimate (9<sup>th</sup>) floor of the TMDI-equipped structure, normalized by the same response quantity of the uncontrolled structure.

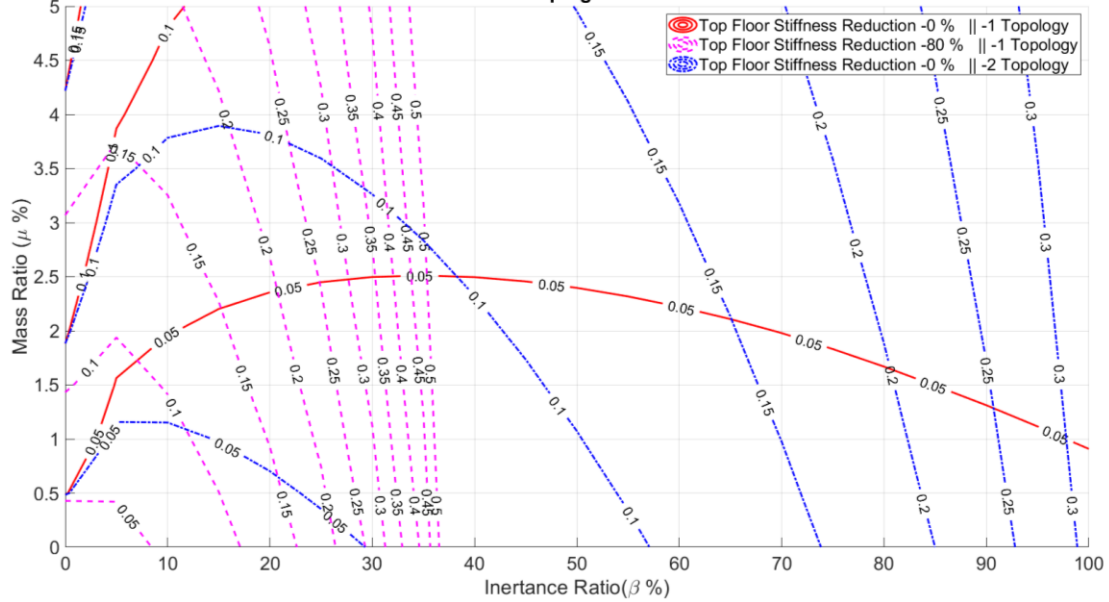


Figure 3 Iso-value optimal damping ratio curves for various TMDI connectivities.

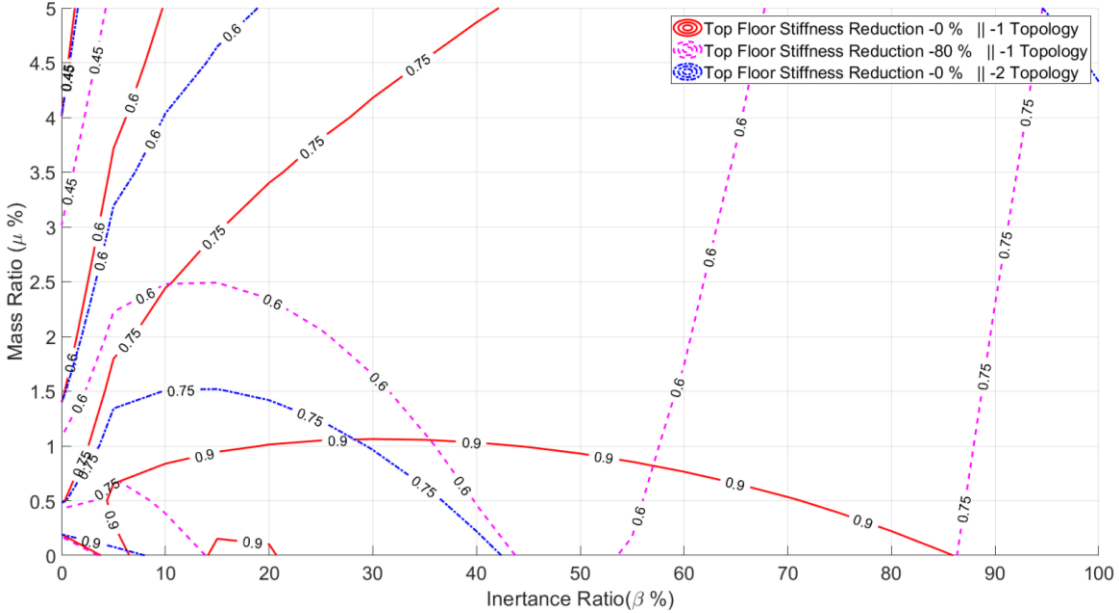


Figure 4 Iso-value curves of displacement variance of the penultimate floor of optimal TMDI-equipped structure over the uncontrolled structure for various TMDI connectivities.

It is seen that trends of iso-value curves of the optimal  $\zeta_{TMDI}$  in Figure 3 between “-2” and “-1” with top-floor softening TMDIs correlate well. In particular, curves become parallel to the y-axis as  $\beta$  increases beyond a critical value. This means that optimal  $\zeta_{TMDI}$  increases monotonically with  $\beta$  for fixed  $\mu$ , and this increase is much more rapid for “-1” with top floor softening, while becoming insensitive to the attached mass. The critical inertance value above which iso-value curves are mostly parallel to the y-axis is smaller for the “-1” TMDI with top floor softening (about 15%) compared to the “-2” TMDI (about 50%). For inertance ratios below these critical values, optimal  $\zeta_{TMDI}$  does depend on the attached mass: it increases monotonically with  $\mu$  for fixed  $\beta$ . Notably, optimal  $\zeta_{TMDI}$  trends for “-1” TMDI with no top floor softening are very different from the

above: they do not vary significantly and they are relatively insensitive with respect to  $\beta$  being mostly dependent on  $\mu$ .

Turning the attention to the normalized OF in Figure 4, interpreted as a TMDI seismic performance index, it is seen that “-2” outperforms “-1” TMDI configuration for any  $\mu$ - $\beta$  combination which confirms previous studies (Giaralis and Taflanidis 2015, 2018). However, the “-1” TMDI with top floor softening outperforms the “-2” configuration demonstrating the usefulness of the herein proposed modification of the primary/host building structure in conjunction with “-1” TMDI configuration. The improved TMDI performance with top floor softening may be attributed to the increased optimal  $\zeta_{TMDI}$  derived from solving the optimization problem in Eq.(9). For example, for the arbitrarily chosen point on the  $\mu$ - $\beta$  plain indicated by a cross in Figures 3 and 4 ( $\mu=0.5\%$  and  $\beta=40\%$ ), the normalized OF values equal to 0.84, 0.68, and 0.56 for “-1”, “-2”, and “-1” with soft top floor, respectively, which correspond to 0.05%, 0.10%, and 0.72% optimal  $\zeta_{TMDI}$ . More importantly, by treating Figure 4 as a design chart within a performance-based design context, the attached weight reduction for fixed performance achieved by the “-1” with soft top floor is readily evident. For illustration, one can trace the 0.6 iso-value curve in Figure 4 (“-1” TMDI with soft top floor) to see that the same performance can be achieved with 1.1% attached mass and no inertance as well as with 0.5% attached mass and 38% inertance. Still, it is also observed in Figure 4 that there is a certain limiting inertance value (about 55%) beyond which any further increase in the inertance becomes detrimental to the performance of the “-1” TMDI configuration with soft top floor. This observation suggests that selection of the inertial TMDI properties in conjunction with top floor softening requires careful consideration. As a final remark, it is seen that the inclusion of the inerter appears to be more beneficial for relatively small attached  $M_{TMDI}$  mass for the case of soft top floor. This trend confirms previously published numerical data involving reliability-based optimum design of TMDIs with no top floor softening (Giaralis and Taflanidis 2015, 2018).

### Performance assessment using Eurocode 8 compatible ground motions

In this section, the effectiveness of “-1” TMDI with soft top floor vis-à-vis “-1” and “-2” TMDI configurations for seismic protection of building structures is further assessed using a suite of 7 recorded ground motions (GMs). Performance is gauged in terms of root mean square (RMS) and peak absolute values for the 9<sup>th</sup> floor deflection, 8<sup>th</sup> floor acceleration, and 9<sup>th</sup> storey drift. Optimal TMDI designs for the previously discussed case with  $\mu=0.5\%$  and  $\beta=40\%$  are examined. The GMs considered are chosen from a databank of 44 far-field GMs used in FEMA P-695 report (FEMA 2009) based on the closeness of their PGA to 0.36g used in the optimal TMDI design. They are identified in the first column of Tables 1 and 2 and they correspond to seismic events of magnitude  $6.9 \leq M \leq 7.4$ , epicentral distance  $7.1 \text{ km} \leq R \leq 19.7 \text{ km}$  and  $0.34 \text{ g} \leq \text{PGA} \leq 0.50 \text{ g}$ . Further, they have been modified to satisfy the Eurocode 8 spectral matching criteria with the target response spectrum in Figure 2(b) via the harmonic wavelet-based approach detailed in Giaralis and Spanos (2009, 2010b).

Earthquake component (seismic event)	RMS deflection of 9th floor			RMS acceleration of 8th floor			RMS storey-drift of 9th floor		
	“-1”	“-1” soft floor	“-2”	“-1”	“-1” soft floor	“-2”	“-1”	“-1” soft floor	“-2”
Hector mine-90° (Hector mine, 1999)	1.09	0.96	1.03	0.99	0.96	0.99	1.11	0.95	1.39
Nishi Akashi-90° (Kobe, 1995)	1.04	0.91	0.99	0.97	0.9	0.97	1.09	0.94	1.37
Duzce-270° (Kocaeli, 1999)	1.02	0.91	0.97	0.96	0.91	0.95	1.07	0.95	1.36
Coolwater, TR (Landers, 1992)	0.97	0.81	0.89	0.95	0.87	0.91	1.05	0.88	1.36
Capitola-90° (Loma Prieta, 1989)	0.83	0.6	0.72	0.86	0.71	0.81	0.9	0.67	1.05
Gilroy array #3-90° (Loma Prieta, 1989)	0.9	0.66	0.76	0.9	0.77	0.83	0.99	0.75	1.23
Abbar- transverse (Manjil, 1990)	0.96	0.82	0.9	0.95	0.91	0.97	1.02	0.85	1.08

Mean	0.97	0.81	0.89	0.94	0.86	0.92	1.03	0.86	1.26
------	------	------	------	------	------	------	------	------	------

Table 1 RMS response quantities for a suite of 7 Eurocode 8 compatible ground motions

Earthquake component (seismic event)	Peak deflection of 9th floor			Peak acceleration of 8th floor			Peak storey-drift of 9th floor		
	“-1”	“-1” soft floor	“-2”	“-1”	“-1” soft floor	“-2”	“-1”	“-1” soft floor	“-2”
Hector mine-90° (Hector mine, 1999)	1.00	0.93	0.98	0.99	0.97	1.02	1.25	1.15	1.38
Nishi Akashi-90° (Kobe, 1995)	1.07	0.88	0.97	1.06	1.15	1.11	1.02	0.74	1.05
Duzce-270° (Kocaeli, 1999)	0.99	0.89	0.95	0.98	0.92	0.98	1.04	0.94	0.89
Coolwater, TR (Landers, 1992)	0.97	0.89	0.92	0.96	1.01	1.02	1.03	0.86	0.8
Capitola-90° (Loma Prieta, 1989)	0.87	0.76	0.86	1.02	0.97	0.98	0.91	0.8	0.82
Gilroy array #3-90° (Loma Prieta, 1989)	1.00	0.93	0.97	0.98	1.00	1.02	0.99	0.82	1.06
Abbar- transverse (Manjil, 1990)	0.96	0.8	0.89	0.95	0.85	0.97	0.97	0.8	0.94
<b>Mean</b>	<b>0.98</b>	<b>0.87</b>	<b>0.93</b>	<b>0.99</b>	<b>0.98</b>	<b>1.01</b>	<b>1.03</b>	<b>0.87</b>	<b>0.99</b>

Table 2 Peak response quantities for a suite of 7 Eurocode 8 compatible ground motions

RMS and peak absolute values of all the examined response quantities for all TMDI equipped structures are reported in Tables 1 and 2, respectively, for each GM normalized by the response of the uncontrolled structure. Mean values from all 7 GMs are also included in the last row of the tables. These results confirm the superiority of “-1” TMDI topology with soft top story which improves on average the performance of the uncontrolled structure by about 20% in terms of RMS displacement and by about 15% in terms of RMS floor acceleration and inter-storey drift. These are about 85% better improvement than the one achieved by the “-2” TMDI configuration. Similarly better improvements are noted in terms of peak responses as well (Table 2). For illustration, Figures 5 and 6 plot response time-histories for one arbitrarily selected GM which verify the improved seismic performance endowed to the uncontrolled structure by “-1” TMDI with soft top floor compared to the “-2” TMDI configuration.

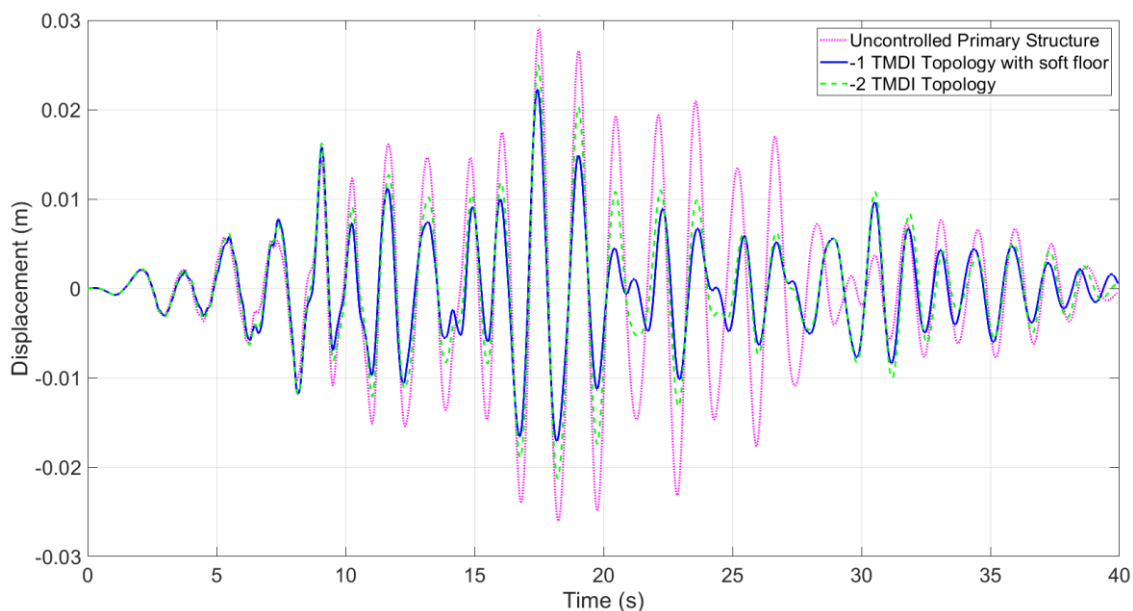


Figure 5 Response history of 9th floor deflection under Capitola-90° GM.

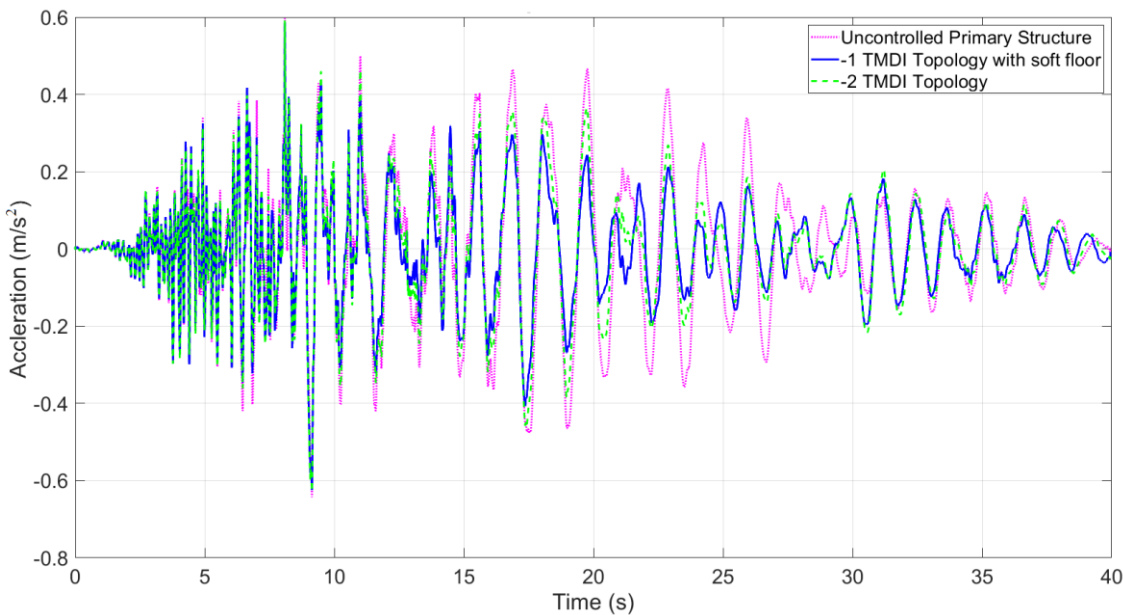


Figure 6 Response history of 8<sup>th</sup> floor acceleration under Capitola-90° GM.

### Concluding remarks

The potential of a novel structural modification, top floor softening, to enhance the performance of TMDI-equipped multi-storey building structures has been numerically assessed. Using a linear 10-storey shear frame as a test-bed, it was found that TMDIs spanning one floor (“-1” TMDI) are more effective than TMDIs spanning two floors (“-2” TMDI) upon top-floor softening by 80%. This was shown by considering “-1” and “-2” TMDIs with wide range of inertial properties optimally tuned to minimize penultimate floor deflection variance for coloured stationary excitation compatible with the Eurocode 8 response spectrum. Moreover, improved performance of “-1” TMDI with top floor softening compared to “-2” TMDI by 85% or more is found in terms of root-mean-square and peak values for penultimate floor deflection, storey drift, and acceleration by considering response history analyses to optimal TMDI-equipped structures for a suite of 7 ground motions spectrally matched to Eurocode 8 response spectrum. In view of the herein furnished results, it is concluded that top-floor softening may improve significantly the seismic performance of TMDI-equipped building structures. Nevertheless, further work is warranted to identify the level of required softening to achieve target performance within a performance-based design context, as well as to account for potential nonlinear structural response and non-ideal inerter behaviour.

### REFERENCES

- De Angelis M, Perno S and Reggio A (2012), Dynamic response and optimal design of structures with large mass ratio TMD, *Earthquake Engineering and Structural Dynamics*, 41:41–60
- BS EN 1998-1:2004+A1:2013, Eurocode 8: Design of structures for earthquake resistance – Part 1: General rules, seismic actions and rules for buildings, AMD 31st May 2013
- FEMA (2009), Recommended Methodology for Quantification of Building System Performance and Response Parameters, FEMA P-695, Redwood City, CA.
- Giaralis A and Spanos PD (2009), Wavelets based response spectrum compatible synthesis of accelerograms-Eurocode application (EC8), *Soil Dynamics and Earthquake Engineering*, 29: 219-235
- Giaralis A and Spanos PD (2010a), Effective linear damping and stiffness coefficients of nonlinear systems for design spectrum based analysis, *Soil Dynamics and Earthquake Engineering*, 30: 798-810

- Giaralis A and Spanos PD (2010b), Derivation of Eurocode 8 spectrum-compatible time-histories from recorded seismic accelerograms via harmonic wavelets, 9<sup>th</sup> HSTAM International Congress on Mechanics, paper #023, pp. 669-677, Limassol, Cyprus.
- Giaralis A and Taflanidis AA (2015), Reliability-based Design of Tuned Mass-Damper-Inerter (TMDI) Equipped Multi-storey Frame Buildings under Seismic Excitation, 12th International Conference on Applications of Statistics and Probability in Civil Engineering, ICASP12 Vancouver, Canada
- Giaralis A and Petrini F (2017), Wind-induced vibration mitigation in tall buildings using the tuned mass-damper-inerter (TMDI), *Journal of Structural Engineering, ASCE*, 143: 04017127
- Giaralis A and Taflanidis AA (2018), Optimal tuned mass-damper-inerter (TMDI) design for seismically excited MDOF structures with model uncertainties based on reliability criteria, *Structural Control and Health Monitoring*, 25: e2082
- Hoang N, Fujino Y and Warnitchai P (2008), Optimal tuned mass damper for seismic applications and practical design formulas, *Engineering Structures*, 30: 707-715
- Lazar IF, Nield SA and Wagg DJ (2014) Using an inerter-based device for structural vibration suppression. *Earthquake Engineering and Structural Dynamics*, 43:1129-1147
- Marian L and Giaralis A (2013) Optimal design of inerter devices combined with TMDs for vibration control of buildings exposed to stochastic seismic excitations. *Proceedings of the 11th ICOSSAR International Conference on Structural Safety and Reliability for Integrating Structural Analysis, Risk and Reliability*, New York, USA, 16-20 June, 1025-1032
- Marian L and Giaralis A (2014) Optimal design of a novel tuned mass-damper-inerter (TMDI) passive vibration control configuration for stochastically support-excited structural systems. *Probabilistic Engineering Mechanics*, 38: 156-164
- Moutinho C (2012), An alternative methodology for designing tuned mass dampers to reduce seismic vibrations in building structures, *Earthquake Engineering and Structural Dynamics*, 41: 2059-2073
- Nakaminami S, Kida H, Ikago K and Inoue N (2016), Dynamic testing of a full-scale hydraulic inerter-damper for the seismic protection of civil structures, 7th International conference on advances in experimental structural engineering, pp. 41-54. DOI:10.7414/7aese.T1.55.
- Papageorgiou C, Houghton NE and Smith MC (2008), Experimental testing and analysis of inerter devices, *Journal of Dynamical Systems, Measurement and Control* 131: 011001.
- Pinkaew T, Lukkunaprasit P and Chatupote P (2003), Seismic effectiveness of tuned mass dampers for damage reduction of structures, *Engineering Structures* 25: 39–46
- Ruiz R, Taflanidis AA, Giaralis A and Lopez-Garcia D (2018), Risk-informed optimization of the tuned mass-damper-inerter (TMDI) for the seismic protection of multi-storey building structures, *Engineering Structures*, 177: 836-850.
- Sadek F, Mohraz B, Taylor AW and Chung RM (1997), A method of estimating the parameters of tuned mass dampers for seismic applications, *Earthquake Engineering and Structural Dynamics*, 26:617-635
- Smith MC (2002), Synthesis of mechanical networks: The Inerter. *IEEE Transactions on Automatic Control*, 47:1648-1662.
- Taflanidis AA, Giaralis A and Patsialis D (2019), Multi-objective optimal design of inerter-based vibration absorbers for earthquake protection of multi-storey building structures. *Journal of the Franklin Institute*, in press, DOI: 10.1016/j.jfranklin.2019.02.022.
- Villaverde R and Koyama LA (1993), Damped resonant appendages to increase inherent damping in buildings, *Earthquake Engineering and Structural Dynamics* 22: 491–508